JOURNAL OF CATALYSIS 114, 354–367 (1988)

The Passivating Oxidation of Platinum

R. W. McCabe,* C. Wong,* and H. S. Woo†

*Physical Chemistry Department, General Motors Research Laboratories, Warren, Michigan 48090-9055, and †Department of Chemical Engineering, Purdue University, West Lafayette, Indiana 47907

Received April 4, 1988; revised June 6, 1988

The oxidation of platinum by gaseous oxygen has been studied for a series of silica and alumina-supported Pt catalysts of widely varying mean particle size. Correlation of the oxidation extent (as measured by temperature-programmed reduction) with mean particle radius (as determined from chemisorption measurements) shows that platinum oxidation is highly passivating, i.e., essentially limited to the surface layer of Pt atoms. Thus the oxidizable fraction of Pt in a catalyst sample is simply proportional to the fraction of surface Pt atoms, which explains why highly dispersed supported Pt samples oxidize more thoroughly than bulk Pt. The passivating nature of Pt oxidation is independent of both the Pt particle size (for bulk Pt down to 0.75-nm-radius particles) and the type of support (no support, silica, or alumina). The detailed structure and chemical identity of the passivating layer could not be identified; in particular, no clear distinction could be made between oxidic and chemisorbed oxygen, especially for particles with radii greater than 2 nm. Highly dispersed samples were more difficult to reduce than low-dispersion samples, possibly owing to an absence of metallic sites for H_2 dissociation in the highly dispersed samples.

INTRODUCTION

The oxidation of platinum has been of catalytic interest since 1922, when Adams and Voorhees first employed bulk Pt oxides for the reduction of organic compounds (*1*). Although characterized by Adams and Voorhees as $PtO_2 \cdot H_2O$, the detailed composition and structure of the so-called "Adams" catalyst have not been resolved (*2–4*). A similar situation exists for the other reported oxides of Pt, namely PtO and Pt_3O_4 (*5–10*). The difficulties encountered in characterizing Pt oxides can be attributed primarily to a combination of poor crystallinity and the presence of impurities (*2, 10, 11*). In particular, Pt forms a wide range of ternary oxides, including the well-known Pt bronzes ($M_xPt_3O_4$ compounds, where M is generally a Group I or II cation and where $0 < x < 1$) (*2, 12*). Adams' catalyst, for example, contains considerable $Na_xPt_3O_4$ owing to its synthesis by reaction of $NaNO_3$ with H_2PtCl_6 (*2*).

In addition to the synthesis of bulk Pt oxides, experiments examining the oxidation characteristics of Pt metal have been carried out. Such experiments have included electrochemical studies, high-temperature (>1100 K) oxidation studies, ultrahigh vacuum (UHV) studies of single-crystal surfaces, and studies of small supported Pt crystallites. Research in these areas is briefly reviewed in the following four paragraphs.

Two recent studies have shown that $Pt(OH)_4$ films are formed during the electrochemical oxidation of Pt in acid electrolyte (*13, 14*). In both studies, compositions of the electrochemical films were compared to the compositions of adsorbed layers obtained by exposing the same single-crystal samples to H_2O and O_2 in UHV. Significant differences were noted, indicating that different processes occur in electrochemical and gas-phase Pt oxidation. For this reason, we confine our attention to the oxidation of Pt by O_2 gas in this paper.

Studies of high-temperature Pt oxidation have focused on the formation of volatile PtO_2 (*15–18*). The PtO_2 molecules thus formed are highly unstable, but can lead to

0021-9517/88 $3.00

significant transport of Pt away from metal surfaces given sufficient time. Thus high-temperature oxidation can be of importance in Pt catalysis as a transport path for catalyst sintering and restructuring (*19–21*). However, this issue will not be addressed in the present paper where we confine our experiments to the temperature range below 875 K where stable Pt oxide phases are formed.

Since 1974, a number of oxidation studies have been carried out on Pt single crystals in UHV. As with bulk PtO_2 chemistry, characterization of oxide films on single-crystal surfaces has been clouded by problems with impurity species and phase identification. For example, a number of early UHV studies reported the formation of a "high-temperature" oxide phase upon exposing Pt crystals to O_2 at temperatures ca. 1000 K (*22–26*). Subsequent studies attributed the high-temperature oxide to impurities (particularly Si) that segregate to the surface and become oxidized during high-temperature O_2 exposure (*27–29*). Another issue raised by single-crystal studies is the distinction between surface Pt oxide phases and chemisorbed O atoms (*14, 30–33*), with some groups reporting Pt oxide formation (*14*) and others chemisorbed oxygen phases (*33*) for experiments carried out with the same crystal faces under similar experimental conditions. In addition to the UHV studies, Pt oxidation has been examined near atmospheric pressure using wire (*34*) and powder (*35, 36*) samples.

The oxidation of supported Pt crystallites has received considerable attention in recent years given the broad use of supported Pt catalysts in hydrocarbon reforming and catalytic combustion. Although only a few studies have focused exclusively on the oxidation behavior of supported Pt (*37–40*), many more have touched on Pt oxidation as it relates to Pt sintering and redispersion (*39, 40–55*), morphology and size distribution of Pt crystallites (*43, 45–49, 56–71*), interactions of Pt with various supports (*37, 38, 45–48, 72*), preparative techniques (chloride effects, etc.) (*39, 49, 65, 71, 73–75*), and activity and selectivity (*35, 36, 76–91*).

Despite the attention Pt oxidation has received, a number of fundamental questions remain: (i) What is the stoichiometry and chemical nature of the oxide phase (i.e., is it PtO, Pt_3O_4, PtO_2, or simply chemisorbed oxygen)? (ii) Can thick films of Pt oxide be produced? (iii) Does the support play a significant role in the oxidation of small Pt crystallites? (iv) Do small Pt particles oxidize and reduce more rapidly and more extensively than large particles? (v) What is the role of impurity species in Pt oxidation? This study addresses the questions above by examining the oxidation characteristics of both bulk Pt samples (powders) and supported Pt catalysts (alumina and silica supports). Through a combination of temperature-programmed reduction, chemisorption measurements, and qualitative X-ray scattering and EXAFS experiments, we show that the oxidation of Pt is highly passivating and essentially limited to the surface layer of Pt atoms regardless of the size and nature (bulk or supported) of the Pt particles. We also provide evidence that the oxide phase formed in particles with radii less than $\approx$0.75 nm is PtO_2, whereas for particles with radii greater than $\approx$2 nm, no clear distinction can be made between chemisorbed and oxidic oxygen.

EXPERIMENTAL

Catalysts

Three supported catalysts were employed: (i) 0.7% Pt on SiO_2, (ii) 5.2% Pt on SiO_2, and 1% Pt on γ-Al_2O_3. The 0.7 and 5.2% Pt on SiO_2 catalysts were prepared by ion exchange of $Pt(NH_3)_4Cl_2 \cdot H_2O$ with Davison 923 silica suspended in an excess of aqueous ammonium hydroxide. The synthesis closely followed the method of Uchijima *et al.* (*65*). The catalysts were then washed with distilled water, dried overnight at 373 K, calcined for 1 h at 393 K in air, and reduced at 573 K for 2 h in flowing 5%

H_2/N_2. The 1% $Pt/\gamma\text{-}Al_2O_3$ catalyst was prepared by impregnating Grace $\gamma\text{-}Al_2O_3$ pellets (3 mm diameter, 145 m^2/g BET area) with a minimum-volume solution of a $Pt_{12}(CO)_{24}$ cluster in tetrahydrofuran. The catalyzed pellets were dried for 24 h at 383 K and then crushed to 100–200 mesh prior to use.

Some experiments were also conducted with Pt and PtO_2 powders obtained from Aldrich Chemicals. Two PtO_2 powders were employed, respectively designated "amorphous" and "crystalline" in the Aldrich catalog (*92*).

Reduction/Oxidation Experiments

Reduction/oxidation experiments were carried out in a temperature-programmed reduction/oxidation (TPR/TPO) apparatus that has been described previously (*93*). The TPR/TPO cell was loaded with 50–200 mg of catalyst powder sandwiched between retaining plugs of quartz wool. Reductions were carried out in 5% H_2/Ar mixtures and oxidations in 5% O_2/He mixtures (premixed gas cylinders from Scott Specialty chemicals; 99.999% Ar and He purity). The 5% H_2/Ar was passed through an Oxysorb trap prior to use and the 5% O_2/He was passed through a Drierite trap. Flow rates were 10 cm^3/min in both cases. The heating rate was 7 K/min in all experiments.

The TPR/TPO cell was used both for the preparation of the oxidized Pt samples and for the subsequent titration of the oxygen content of the oxidized samples. The procedure was as follows:

- The fresh catalyst was first reduced for 2 h at 773 K in the H_2/Ar feed to ensure that precursor species would be decomposed.
- The catalyst was then treated for 2 h in flowing O_2/He at one of three temperatures (573, 723, or 873 K) to effect different Pt dispersions. These oxidizing pretreatments are called "sintering" treatments throughout this report.
- The catalyst was subsequently ramped to 773 K in flowing H_2/Ar (this ensured complete reduction since TPR showed no H_2 uptake for any of the samples above 500 K).
- The catalyst was then exposed to flowing O_2/He at 573 K for 2 h (this is designated the "standard" oxidation treatment throughout this report).
- A TPR trace was then obtained starting from 123 K. The amount of oxide was determined from the area under the TPR trace after subtracting the background associated with H_2 uptake on the blank support.

The integrated H_2 uptakes in the TPR experiments were calibrated from TPR profiles of CuO and PtO_2 standards.

In addition to the 2-h oxidations carried out in the TPR/TPO apparatus, some long-term oxidations were carried out in a tube furnace. The catalyst samples were loaded in an alumina boat and placed in the tube furnace where they were heated for periods up to 260 h in a flowing stream of pure O_2. A bed of Pt/Al_2O_3 catalyst was positioned upstream from the samples to oxidize any reducing agents that might be present as impurities in the O_2 stream.

Chemisorption Measurements

Pt dispersions were calculated from static CO chemisorption measurements made with a Micromeritics ChemiSorb 2800 automated chemisorption analyzer. The chemisorption measurements were performed on the samples after they had been sintered and analyzed by TPR. Each sample was then loaded into the chemisorption analyzer and conditioned as follows prior to the chemisorption measurements: (i) air at 573 K for 1 h, (ii) 5% H_2 at 573 K for 1 h, and (iii) 2-h evacuation at 10^{-3} mm Hg at 573 K (this conditioning procedure was sufficiently mild that it did not change the oxidation characteristics of the samples). The irreversible CO uptake was then obtained by the standard method of first measuring the total uptake at 308 K, then pumping out the cell, and redosing with CO to obtain the reversible component. The irreversible CO

uptake was then obtained as the difference between the total and the reversible uptakes.

A CO-to-Pt ratio of 1 was assumed for the dispersion calculations. Some chemisorption measurements were also made with H_2. The calculated dispersions based on H_2 chemisorption (assuming an H/Pt ratio of 1) agreed well with the CO numbers for the low-dispersion catalysts, but the H uptakes were much greater than the CO uptakes for the highly dispersed samples, even providing H/Pt ratios approaching 1.5 for the most highly dispersed samples (compared to a maximum CO/Pt of 0.83). The high H/Pt ratios could result from multiple H atom adsorption per Pt atom or spillover of H atoms onto the support. Such complications were not present in the CO chemisorption data.

X-Ray Diffraction and EXAFS Experiments

Qualitative experiments were undertaken with the 1% Pt/γ-Al_2O_3 catalyst at the Brookhaven National Synchrotron Light Source utilizing anomalous X-ray scattering (Station X-18a) and extended X-ray absorption fine structure (EXAFS) (Station X-18b). In both cases, spectra were obtained near the Pt L_{III}-edge in air at room temperature. The anomalous scattering experiments involved scanning in 2θ increments of 0.05° between 15° and 35° (2θ). Sequential scans were obtained at photon energies of 11,516 and 11,416 eV. EXAFS data were obtained for Pt foil and PtO_2 in addition to the 1% Pt/γ-Al_2O_3 powder sample.

RESULTS

Sintering Pretreatments

As noted above, the catalysts were pretreated by heating in flowing 5% O_2/He for 2 h at varying temperatures to effect a broad range of mean particle sizes prior to the TPR and CO chemisorption experiments. The results of these sintering pretreatments are given in Table 1. The fraction of exposed Pt atoms (i.e., dispersion) is shown to range from 0.18 to 0.83 for the various samples. For all three catalyst formulations, the dispersion decreased only slightly by sintering at 723 K compared to 573 K, but significant decreases in dispersion were effected by sintering at 873 K. The catalysts were thoroughly reduced and reoxidized under the standard condition of 573 K prior to the TPR experiments presented below.

TABLE 1

Effect of Sintering on Fraction-Exposed (D_M)[a]

Catalyst	T_S	D_M
0.7% Pt/SiO_2	573	0.83
0.7% Pt/SiO_2	723	0.82
0.7% Pt/SiO_2	873	0.51
5.2% Pt/SiO_2	573	0.70
5.2% Pt/SiO_2	723	0.67
5.2% Pt/SiO_2	873	0.28
1.0% Pt/Al_2O_3	573	0.46
1.0% Pt/Al_2O_3	723	0.40
1.0% Pt/Al_2O_3	873	0.18

[a] Samples heated in flowing 5% O_2/He for 2 h at indicated temperatures (K).

TPR Experiments

Figure 1 shows TPR profiles for the three sintered samples of the 5.2% Pt/SiO_2 catalyst after the standard 573 K oxidation treatment. The maximum in the TPR profile shifted to lower temperatures and the peaks narrowed as the sintering temperature was increased. The reduction profiles progressed from a single broad peak centered near 330 K (for T_S = 573 K; D_M = 0.70) to two poorly resolved peaks at 235 and 295 K (for T_S = 723 K; D_M = 0.67) to a single low-temperature peak near 200 K (for T_S = 873 K; D_M = 0.28).

The 0.7% Pt/SiO_2 and 1% Pt/Al_2O_3 catalysts showed TPR trends similar to those of the 5.2% Pt/SiO_2 catalyst with increasing sintering temperature. The reduction peaks

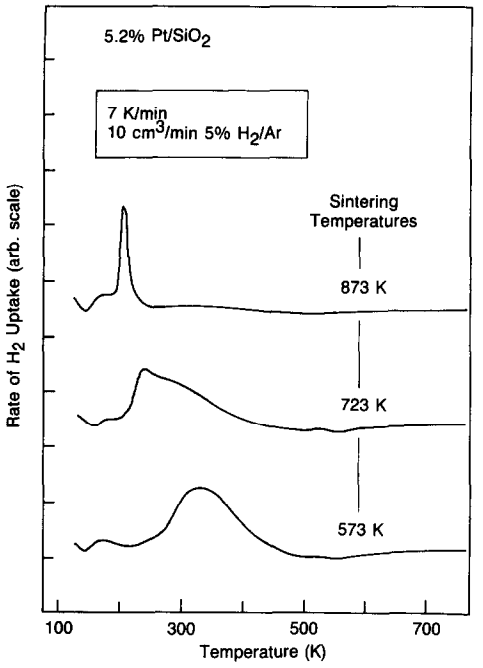

FIG. 1. A series of TPR profiles for the 5.2% Pt/SiO_2 catalyst after sintering in 5% O_2/He for 2 h at 573, 723, and 873 K. The TPR profiles were obtained after reducing the sintered catalysts (by ramping to 773 K in 5% H_2/Ar) and reoxidizing in 5% O_2/He for 2 h at 573 K. The TPR profiles were obtained at 7 K/min heating rate and 10 cm^3/min of 5% H_2/Ar. The curves are arbitrarily positioned on the y-axis but are scaled identically.

narrowed and shifted to lower temperatures, and the H_2 uptake decreased as the sintering temperature was increased. Representative TPR profiles are shown in Fig. 2 for the 1% Pt/Al_2O_3 catalyst after sintering at 723 and 873 K (the profile after 573 K sintering was similar to the 723 K profile). Note that the 1% Pt/Al_2O_3 catalyst showed poorly resolved peaks near 250 and 350 K after 723 K sintering, similar to those observed for the 5.2% Pt/SiO_2 catalyst. Also, sintering at 873 K resulted in a TPR profile with only a single feature near 230 K, again similar to the 5.2% Pt/SiO_2 catalyst.

An additional experiment was undertaken to determine whether the oxygen taken up by the catalysts during the standard oxidation at 573 K (prior to the TPR runs) was present as oxide or chemisorbed oxygen. To produce a chemisorbed layer, a 0.7% Pt/SiO_2 catalyst was sintered at 573 K and then reduced at 773 K, cooled to 173 K in flowing Ar, and then exposed to 5% O_2/He for 1 h at 173 K (O_2 is known to chemisorb dissociatively on Pt above 150 K (*30, 94*). A TPR run was made after the 173 K O_2 exposure. The TPR profile showed only a single peak near 200 K; it lacked the higher temperature features observed for the 573 and 723 K sintered catalysts after the standard 573 K oxidation. However, the 200 K TPR peak observed after the 173 K O_2 exposure was coincident with the TPR peak observed for the 873 K sintered catalysts, thereby raising the possibility that the O_2 uptake by the 873 K sintered catalysts during the standard 573 K oxidation could be due to chemisorption.

For simplicity, we refer to the O_2 uptake as oxidation throughout this paper, even though it is possible that both oxidic and chemisorbed oxygen species may form over the broad range of particle sizes examined in this study. The distinction between

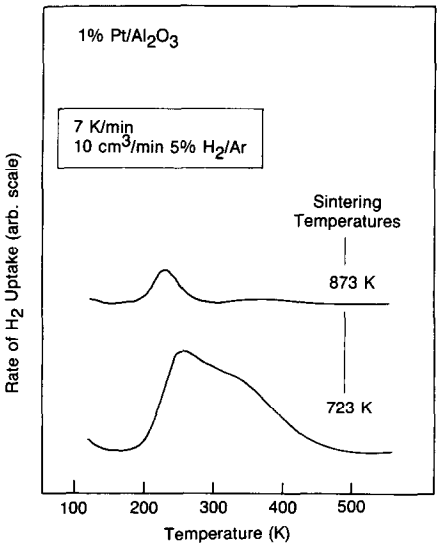

FIG. 2. TPR profiles for the 1% Pt/Al_2O_3 catalyst after sintering at 723 and 873 K. The sintering and TPR procedures were identical to those in Fig. 1. The curves are arbitrarily positioned on the y-axis but are scaled identically.

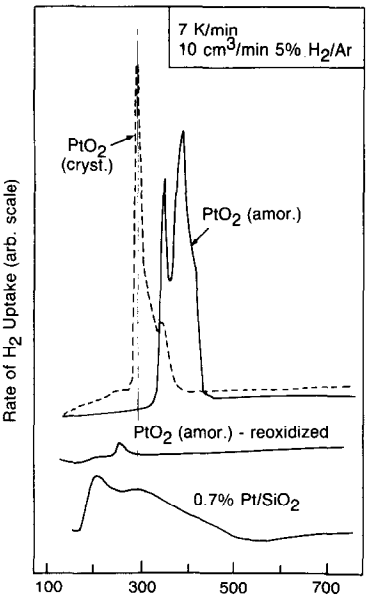

FIG. 3. TPR profiles (from top to bottom) of (i) a 2.7-mg sample of crystalline PtO_2 (dashed curve), (ii) a 3.7-mg sample of amorphous PtO_2, (iii) the same sample of amorphous after complete reduction to Pt and reoxidation in 5% O_2/He for 2 h at 573 K, and (iv) a sample of 0.7% Pt/SiO_2 catalyst after sintering at 573 K. The curves are arbitrarily positioned on the y-axis but are scaled identically.

chemisorbed and oxidic oxygen will be considered in more detail under Discussion.

Figure 3 compares the TPR profile of the 0.7% Pt/SiO_2 catalyst (after sintering at 573 K) with TPR profiles of "crystalline" and "amorphous" PtO_2. The PtO_2 profiles differ significantly, but both show appreciable H_2 uptake only at temperatures above 290 K. The TPR peaks for the bulk PtO_2 samples occur over the temperature range where the broad high-temperature feature is observed in the 0.7% Pt/SiO_2 TPR profile. Specifically, it can be seen from Fig. 3 that the 290 K peak in the crystalline PtO_2 profile is coincident with the maximum in the high-temperature TPR feature of the 0.7% Pt/SiO_2 sample. Figure 3 also shows a TPR profile obtained after reducing the amorphous PtO_2 and subsequently exposing it to O_2 under our standard conditions (10 cm^3/min of 5% O_2/He for 2 h at 573 K). A single weak TPR feature was observed near 260 K, the integrated H_2 uptake of which amounted to less than 4% of the initial uptake for the amorphous PtO_2 sample.

Figure 4 shows results of experiments carried out to assess the effects of oxidation temperature on the subsequent reduction characteristics of the 5.2% Pt/SiO_2 catalyst. For sintering temperatures of 723 and 873 K, TPR profiles were obtained directly after sintering (dashed curves) and after complete reduction and reoxidation at 573 K (solid curves). The dashed curves are slightly displaced in the vertical direction relative to the solid curves for clarity. At both sintering temperatures, a downward shift of about 15 K was observed in the peak locations for the 573 K oxidized catalyst compared to the catalyst oxidized at the sintering temperature. Also, for the 723 K sintering temperature, the two TPR

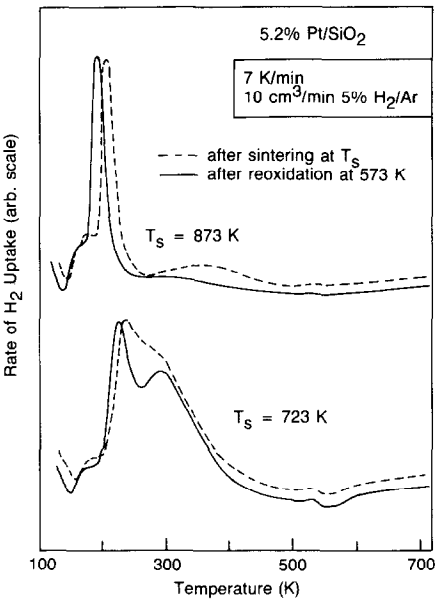

FIG. 4. TPR profiles for the 5.2% Pt/SiO_2 catalyst after sintering at 723 and 873 K. Two TPR profiles are shown for each sintering temperature: the dashed curve is the TPR profile obtained directly after the sintering treatment, and the solid curve is the TPR profile obtained after reducing the sintered catalyst and then reoxidizing for 2 h at 573 K. The curves are arbitrarily positioned on the y-axis but are scaled identically.

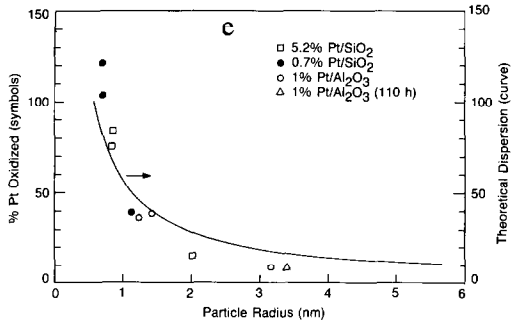

FIG. 5. A plot of percentage Pt oxidized (as determined by H_2 uptakes during TPR) vs Pt particle radius (as determined by CO chemisorption) for the 0.7% Pt and 5.2% Pt on silica catalysts and the 1% Pt on alumina catalyst after various sintering treatments. The catalysts were all oxidized at 573 K for 2 h prior to TPR analysis with the exception of the sample designated with the triangle. It was oxidized for an additional 110 h in pure O_2 at 573 K prior to TPR analysis.

peaks were better resolved after reoxidation at 573 K. Note, however, that the integrated H_2 uptakes given by the areas under the curves were virtually identical irrespective of whether the catalyst was exposed to O_2 at the sintering temperature or at 573 K. Thus the uptake of O_2 is not affected by temperature over the 573–873 K range.

Comparison of TPR and CO Chemisorption Data

The total H_2 uptakes associated with reduction of the oxidized Pt samples were determined by integrating the areas under the TPR traces after correcting for H_2 uptake associated with the blank support. The oxidized fraction of the Pt in each sample was then calculated from the TPR H_2 uptakes, assuming (i) each O atom reacts with one H_2 molecule to produce one H_2O molecule, and (ii) the oxide stoichiometry is that of PtO_2 (i.e., two O atoms per Pt atom). Figure 5 shows a plot of the oxidized fraction of each catalyst vs mean particle radius. The mean particle radius was determined from the CO chemisorption measurements on the fully reduced catalysts. The irreversible CO uptake was first divided by the total number of Pt atoms to obtain the fraction of exposed Pt atoms (i.e., metal dispersion, D_M). The volume–area mean particle radius was then calculated from the following relationship for spherical particles,

$$\bar{r}_{va} = \frac{\Sigma_i V_i}{\Sigma_i A_i} = 3\left(\frac{(v_m/a_m)}{D_M}\right), \qquad (1)$$

where v_m is the volume per bulk Pt atom, and a_m is the area per surface Pt atom (*95*).

The solid curve in Fig. 5 is a plot of the particle size–dispersion relation given in Eq. (1). The close fit of Eq. (1) to the data of Fig. 5 indicates that the extent of oxidation tracks dispersion; i.e., only exposed Pt atoms are oxidized.

Most of the points in Fig. 5 lie below the dispersion relation, indicating that, on average, less than a monolayer of Pt is oxidized to PtO_2. In fact, the samples in Fig. 5 with mean particle radii greater than 2 nm yielded O_2 uptakes corresponding to approximately a 1/1 ratio between O atoms and exposed Pt atoms, which would correspond to conversion of either one-half of the exposed Pt atoms to PtO_2 or all of the exposed atoms to a stoichiometric equivalent of PtO. Samples with mean particle radii below 2 nm, however, gave O_2 uptakes that corresponded closely to stoichiometric conversion of the Pt surface atoms to PtO_2. The only exceptions were the two most highly dispersed samples which showed apparent oxidation exceeding 100% conversion of all of the Pt atoms in the samples to PtO_2 (see Fig. 5). The latter is physically unrealistic and may indicate a problem with H_2 spillover onto the SiO_2 support during the TPR experiment. H_2 spillover has been reported on Pt/SiO_2 catalysts in the temperature range of the TPR experiments (*96, 97*) and would be expected to be most significant for highly dispersed catalysts. Additionally, the presence of a spillover effect in TPR is also consistent with our observation that H_2 chemisorption on the same samples yielded apparent dispersions in excess of 100%. Note that any contribution due to H_2 spillover during TPR only serves to increase the apparent extent of oxidation; the

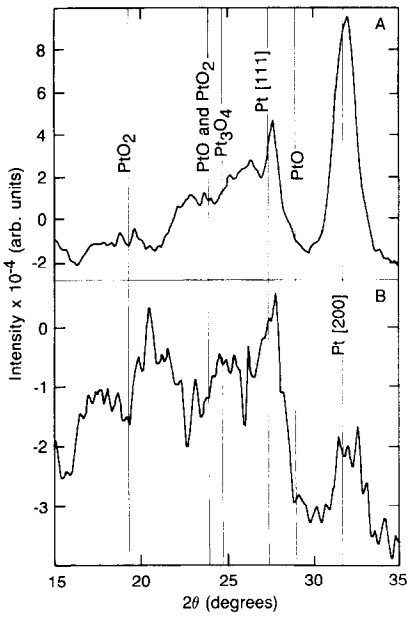

FIG. 6. Intensity vs scattering angle plots for anomalous x-ray scattering experiments carried out with 873 K-sintered samples of 1% Pt/Al_2O_3 prepared from (A) $Pt(NH_3)_4Cl_2$ and (B) $Pt_{12}(CO)_{24}$. The scattering angles associated with major diffraction features of Pt and various Pt oxides are indicated by the vertical lines.

presence or absence of spillover does not modify our conclusion that oxidation is limited to a monolayer equivalent of Pt atoms at most (at least for particles with radii greater than ≈0.75 nm).

The effect of O_2 exposure time on extent of oxidizability was examined for the 1% Pt/Al_2O_3 catalyst. The catalyst was sintered at 873 K, reduced, and reoxidized under standard conditions to yield the data point at 3.2 nm in Fig. 5. The same sample was then exposed to pure O_2 at 573 K for an additional 110 h and then reanalyzed by TPR and chemisorption. The chemisorption analysis indicated a slight increase in mean particle radius by about 0.2 nm, but the TPR analysis showed no additional O_2 uptake beyond that obtained during the first 2 h of oxidation at 573 K. Similar results were obtained during long-term oxidation experiments with bulk Pt samples. For example, a sample of Pt black was initially reduced and then exposed to pure O_2 at 823 K for 120 h. Subsequent TPR analysis showed only trace H_2 uptake thereby confirming that bulk oxidation of Pt cannot be effected even at relatively high temperatures in pure O_2 for many hours.

X-Ray Diffraction and EXAFS

Figure 6 shows anomalous X-ray scattering results obtained for two samples of 1% Pt/Al_2O_3 catalyst—one prepared using $Pt(NH_3)_4Cl_2$ as a precursor (A) and the other prepared with a $Pt_{12}(CO)_{24}$ complex (B). Both catalysts were sintered at 873 K prior to analysis. The difference patterns were of low intensity, and only the most prominent diffraction features, namely the Pt[111] and Pt[200] lines, could be clearly identified. Locations of major diffraction features for various bulk Pt oxides are also indicated in Fig. 6, but none can be readily associated with the rather structureless patterns obtained with either catalyst over the 15–35° 2θ scattering range. The anomalous scattering data simply confirm the conclusion reached on the basis of the combined TPR and chemisorption measurements; i.e., metallic Pt is still present after 2 h exposure to O_2 at 873 K.

Raw EXAFS data are shown in Fig. 7 for the 873 K oxidized 1% Pt/Al_2O_3 catalyst as well as Pt foil and PtO_2. The purpose of the EXAFS experiments was to try to identify the Pt phases present in the supported catalyst. Thus we rely on qualitative fingerprint comparisons between the supported catalyst and reference spectra in the near-edge and extended X-ray regions. In the near-edge region, the white-line intensity of the Pt foil is small relative to the absorption background, whereas the white-line intensity of the PtO_2 sample is large relative to the background. The ratio of white-line to background intensities in the supported Pt sample is between those of Pt and PtO_2, suggesting that the supported sample contains a mixture of Pt and PtO_2 phases. In the extended absorption region, weak features are observed for the supported Pt that are close to features present in both Pt and

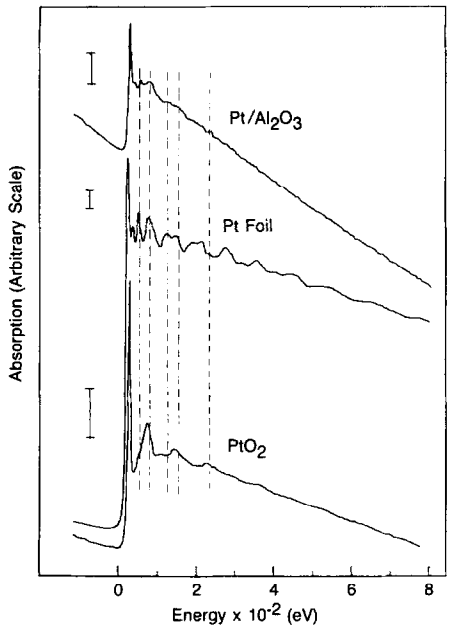

FIG. 7. X-ray absorption intensity vs incident X-ray energy (referenced to the Pt L_{III}-edge). Data are shown for an 873 K-sintered 1% Pt/Al_2O_3 catalyst, Pt foil, and PtO_2. The spectra are scaled differently, with the height of an absorption unit given by the scale bar to the left of each spectrum. The dashed vertical lines are drawn through extended X-ray absorption features observed in the Pt/Al_2O_3 catalyst.

PtO_2, again suggesting a combination of metal and oxide.

DISCUSSION

TPR Data

The TPR data of this study are in good general agreement with other TPR studies of supported Pt catalysts (*37–39, 60, 72, 74, 98*). An exception is that other studies have reported TPR peaks at temperatures between 530 and 570 K (*37–39, 60, 72, 74, 98*)—significantly higher than reported in this study. Although such high-temperature peaks were not observed in our study after the standard pretreatment (which included a 773 K reduction), they were observed for the fresh 1% Pt/Al_2O_3 catalyst when it was not prereduced at 773 K prior to 573 K O_2 exposure and subsequent TPR analysis. Lieske *et al.* (*39, 40*) have clearly associated these high-temperature peaks with the reduction of Pt oxychloride compounds, namely $[Pt^{IV}(OH)_xCl_4]$ and $[Pt^{IV}O_xCl_y]$, produced either during the oxidative decomposition of H_2PtCl_6 or by reaction of Pt atoms with Cl ions in the alumina. Since our Pt/Al_2O_3 catalyst was prepared from a nonchloride-containing Pt cluster compound, the support would appear to be the source of Cl ion in our study. Alternatively, Park *et al.* (*38*) have proposed that high-temperature TPR features arise from the interaction of isolated Pt atoms with a variety of strong acid sites (not just Lewis sites produced by the interaction of Cl anions with uncoordinated Al cations). In either case, we attribute TPR features occurring above 500 K to the reduction of inorganic Pt complexes. Such complexes are decomposed when the samples are reduced at 773 K. Presumably the decomposition of the inorganic Pt complexes is accompanied by the nucleation of Pt particles since the complexes cannot be reformed by subsequent heating in either H_2 or O_2 (*37–39*). The following discussion is thus restricted to the oxidation behavior of *nucleated* Pt, ranging from bulk samples (powders, wire, foils, etc.) to supported crystallites with mean radii down to $\approx$0.75 nm.

The TPR data of Figs. 1–3 argue against an effect of either support on the oxidation characteristics of Pt crystallites. TPR features of the supported catalysts always occurred at temperatures the same as, or lower than, those of the bulk PtO_2 oxides, thereby indicating no support-induced stabilization of Pt oxide. Furthermore, the alumina- and silica-supported catalysts displayed similar TPR profiles, in both the shapes of the profiles and the shifts to lower temperature with increasing sintering temperature. Finally, quantitative O_2 uptakes depended solely on Pt dispersion and not on the type of support, as indicated by the fact that the Pt/SiO_2 and Pt/Al_2O_3 data lie on the same curve in Fig. 5.

The shift of the TPR peaks to lower temperatures with increasing sintering temper-

ature has been observed by other groups (*37–39, 60, 72, 98*). Huizinga *et al.* (*37*) suggested that large oxidized Pt particles reduce more readily because they contain a greater density of sites capable of adsorbing and dissociating H_2 than do small oxidized particles. In a similar vein they proposed that passivated samples (i.e., those covered with a thin oxide film) reduce at low temperatures because H_2 readily diffuses through the oxide film and dissociates at metal sites. Uchijima *et al.* (*65*) examined the reduction kinetics of Pt/SiO_2 catalysts that had been stored in air for long periods. Removal of adsorbed oxygen by pulses of H_2 at 298 K was much more rapid for low-dispersion catalysts than for high-dispersion catalysts. They concluded that the lower reactivity of the highly dispersed catalysts was due to the presence of a more continuous oxygen film in those samples compared to the low-dispersion samples. In our study, all samples with mean dispersions of 40% or greater showed a high-temperature feature between 300 and 350 K; most of those samples displayed a lower-temperature peak as well. The dual peaks observed in the highly dispersed samples suggest a broad range of particle sizes. Since the high-temperature feature occurs in the same temperature range as reduction of bulk PtO_2, we associate it with the reduction of fully oxidized Pt particles. Note that this association with bulk PtO_2 is made on the basis of *reduction kinetics* rather than *particle size*. In fact, the arguments for passivating oxidation that follow in the next section indicate that only those particles with radii less than $\approx$0.75 nm will be completely oxidized; it is this common feature of complete oxidation, rather than particle size, that leads to similar reduction kinetics for large, chemically prepared, bulk PtO_2 particles on the one hand and small supported PtO_2 particles on the other hand. Large supported Pt particles will contain a core of metal atoms after oxidation that, according to Huizinga *et al.* (*37*), will increase the rate of reduction by promoting H_2 adsorption, dissociation, and reaction. Note that we cannot determine the structural relationship between oxide and metal sites in these larger particles. For example, our experiments cannot distinguish between the possibilities that (i) reduction is accelerated by defects in the oxide layer that expose metallic sites, and (ii) the oxide film is continuous over the surface of the particles, but permeable enough to allow rapid diffusion of H_2 to underlying metallic sites where dissociation occurs readily.

The simultaneous presence of oxide and metal sites is not the only possible explanation for the more rapid reduction of large particles than of small particles. As noted previously, the high-temperature sintered, low-dispersion catalysts showed reduction peaks in the same temperature range as chemisorbed oxygen, thus raising the possibility that the oxygen surface film on large Pt particles is chemisorbed oxygen rather than Pt oxide. In that case, the shift of the TPR reduction peaks to lower temperatures with increasing particle size could simply indicate a shift from oxidic to chemisorbed oxygen, with the chemisorbed oxygen being more reactive with H_2 than the oxide.

Passivation

The data of Fig. 5 show that the fraction of Pt that is oxidized decreases precipitously with increasing particle size—ranging from essentially complete oxidation for particles with radii less than $\approx$0.75 nm to less than 10% for particles with radii greater than 3 nm. The decrease in oxidizability with increasing particle size closely tracks the decrease in the fraction of exposed Pt atoms, as indicated by the close correspondence between the data points and the theoretical dispersion curve in Fig. 5. On average, only exposed Pt atoms are oxidized, as indicated by the fact that the data points lie on or below the theoretical dispersion curve. Thus the greater oxidizability of small Pt particles is primarily due to their larger fraction of exposed atoms.

The oxidation of Pt is highly passivating;

oxidation proceeds rapidly to at most a monolayer equivalent of Pt atoms and stops. Deeper oxidation could not be effected by varying the O_2 exposure time, temperature, or O_2 pressure over the range of conditions examined in this study. Thus the 1% Pt/Al_2O_3 catalyst showed the same extent of oxidation after 110 h in pure O_2 at 573 K as after 2 h in 5% O_2 at 573 K (Fig. 5). Similarly, the 5.2% Pt/SiO_2 catalyst showed the same extent of oxidation regardless of whether the O_2 uptake was measured by TPR directly after sintering treatments in O_2 at 723 and 873 K or after a subsequent reduction and reoxidation at 573 K (Fig. 4). The latter experiment indicates that, although the temperature of O_2 exposure affects the *overall* extent of oxidation by changing the dispersion, the *normalized* O_2 uptake (uptake per surface Pt atom) is independent of temperature over the 573–873 K range and is limited to at most a monolayer equivalent of Pt atoms.

Qualitative support for the passivation model of Pt oxidation is contained in the anomalous X-ray scattering and EXAFS data. Both techniques provided evidence for metallic Pt after 1% Pt/Al_2O_3 catalysts had been sintered at 873 K and cooled to room temperature in air. In addition, the EXAFS data showed features characteristic of both metal and oxide phases. A number of other groups have examined air-exposed catalysts by EXAFS (*45, 68, 70, 75*) and X-ray diffraction (*59, 62, 66, 75*). Results have been mixed, with some groups reporting essentially complete oxidation of Pt crystallites (*68, 70*) and others reporting mixtures of metallic and oxidic phases (*45, 75*). The studies reporting complete oxidation involved catalysts prepared and pretreated in such a way that inorganic Pt complexes may have been present. A study by Nandi *et al.* (*75*) closely parallels the results of this study. They reported that air exposure of a 63.5% exposed Pt catalyst produced crystallites with oxide surfaces and metal cores, while an 81% exposed catalyst was nearly fully oxidized.

The passivation model of Pt oxidation applies not only to supported Pt catalysts but also to bulk Pt. Our attempts to reoxidize reduced samples of Pt black and PtO_2 powders always yielded O_2 uptakes corresponding to only monolayer involvement of the Pt, even after times in excess of 250 h. Similar conclusions have been reached by Turner and Maple (*36*) for Pt powder and by Peuckert and Bonzel (*14*) for a Pt[111] single crystal. To our knowledge, the only exception to the monolayer-type passivating oxidation of Pt is the study by Berry (*34*), where thick (ca. 90-nm) films of PtO_2 were reported after long-term oxidation of Pt wires in 1 atm O_2. Berry's results could have been influenced by impurities, however, since surface composition was not monitored, and since the wires were "stabilized" by pretreating in air at 1023–1173 K for 10 h or more. Such pretreatments are known to promote the surface segregation of Ca, Si, P, and S impurities in bulk Pt samples (*28*).

Nature of the Passive Oxygen Film

Although the concept of a passive oxygen film, preventing bulk Pt oxidation, appears generally applicable for Pt particles ranging in size from monolithic single crystals to ≈0.75-nm-radius crystallites, it is not clear whether the chemical nature of the film is identical over such a size range. In particular, it is difficult to distinguish between a passive oxide film and a passivating layer of chemisorbed oxygen. For the most highly dispersed samples of this study, the combination of the 2/1 O-to-Pt stoichiometry from TPR, together with the close correspondence of the reduction temperature to that of bulk PtO_2, suggests that PtO_2 is formed. For particles with radii greater than about 2 nm, however, the lower O-to-Pt stoichiometry (≈1/1), together with the downshift in the TPR peak to ≈200 K (where a peak was also observed for chemisorbed oxygen), raises the possibility that the oxygen surface film may be chemisorbed oxygen rather than platinum oxide.

In particular, the oxygen uptakes for the 2-nm-radius and larger particles are close to those observed by Derry and Ross (*33*) for Pt[100] and Pt[111] single crystals after O_2 exposure at 10^{-3} Pa and 570 K. Despite the relatively high oxygen coverages obtained under their dosing conditions (estimated at $0.75–1.25 \times 10^{15}$ O atoms/cm^2 vs $\approx 0.25 \times 10^{15}$ O atoms/cm^2 under normal UHV dosing conditions of 10^{-5} Pa and 300 K), they concluded from angle-resolved UPS data that the oxygen was chemisorbed and not oxidic. Moreover, they found no evidence for significant penetration of oxygen into the bulk and concluded that place-exchange-type restructuring of the surface, if occurring at all, would be limited to the first two atomic layers. The conclusions of Derry and Ross would appear to apply equally well to the observations of this study, at least for Pt powders and supported crystallites with radii greater than 2 nm. Although we have shown the passivating nature of Pt oxidation to persist over a broad range of particle sizes, the detailed structure and chemical identity of the passive layer still remain to be determined.

CONCLUSIONS

The following conclusions are reached for the oxidation of *metallic* Pt. In general, different results obtain when Pt is in the form of inorganic compounds (e.g., as Pt oxychloride complexes on alumina, or as ternary oxide phases).

- Pt oxidation is highly passivating; the oxide film thickness is less than or equal to one monolayer equivalent of Pt atoms, regardless of O_2 pressure (0.05–1.0 atm), temperature (573–873 K), or length of O_2 exposure (2–250 h).
- Since only exposed Pt atoms are oxidized, the extent of oxidation closely tracks the increase in dispersion that occurs with decreasing particle size. This explains why small supported Pt crystallites are more thoroughly oxidized than either large crystallites or bulk Pt samples (i.e., the small crystallites have larger surface-to-bulk atom ratios).
- The passivating (i.e., monolayer) oxidation of Pt is independent of the type of support (alumina, silica, unsupported). This has been confirmed for bulk Pt powder samples as well as alumina- and silica-supported Pt catalysts with mean particle radii as small as 0.75 nm.
- Reduction kinetics of Pt oxide particles depend strongly on particle size; samples with mean particle radii of 2 nm or greater reduce at temperatures 100–150 K lower than particles with mean particle radii less than ≈ 0.75 nm.
- The detailed structure and chemical nature of the oxide film could not be unequivocally identified. For particles with radii less than ≈ 0.75 nm, the oxygen film appears to be PtO_2 based on TPR H_2 uptakes and peak temperatures close to those of bulk PtO_2. For particles with radii greater than 2 nm, the oxygen film could be chemisorbed oxygen, as suggested by a decrease in O-to-Pt stoichiometry to $\approx$1-to-1 and a concomitant shift in the TPR peak to low temperatures characteristic of chemisorbed oxygen.

ACKNOWLEDGMENTS

We are grateful to Michael G. Zammit and Michael J. D'Aniello, Jr. for preparing the catalysts and carrying out the chemisorption measurements.

REFERENCES

1. Adams, R., and Voorhees, V., *J. Amer. Chem. Soc.* **44,** 1683 (1922).
2. Cahen, D., and Ibers, J. A., *J. Catal.* **31,** 369 (1973).
3. Carswell, L. R., and Schuetz, R. D., *Iowa Acad. Sci.* **68,** 272 (1945).
4. Sukhotin, A. M., Gankin, E. A., Kondrashov, Y. D., Omel'chenko, Y. A., and Shal'man, B. Y., *Russ. J. Inorg. Chem.* **16,** 1690 (1971).
5. Galloni, E. E., and Roffo, A. E., Jr., *J. Chem. Phys.* **9,** 875 (1941).
6. Busch, R. H., *Z. Naturforsch* **56,** 130 (1950).
7. Galloni, E. E., and Busch, R. H., *J. Chem. Phys.* **20,** 198 (1952).
8. Hecq, M., and Hecq, A., *J. Less-Common Met.* **56,** 133 (1977).

9. Cohen, D., Ibers, J. A., and Wagner, J. B., Jr., *Inorg. Chem.* **13,** 1377 (1974).
10. Muller, O., and Roy, R., *J. Less-Common Met.* **16,** 129 (1968).
11. Waser, J., and McClanahan, E. D., Jr., *J. Chem. Phys.* **20,** 199 (1952).
12. Hoekstra, H. R., Siegel, S., and Gallagher, F. X., *Amer. Chem. Soc. Adv. Chem. Ser.* **98,** 39 (1971).
13. Wagner, F. T., and Ross, P. N., Jr., *Appl. Surf. Sci.* **24,** 87 (1985).
14. Peuckert, M., and Bonzel, H. P., *Surf. Sci.* **145,** 239 (1984).
15. Alcock, C. B., and Hooper, G. W., *Proc. R. Soc. London A* **254,** 551 (1960).
16. Fryberg, G. C., and Petrus, H. M., *J. Electrochem. Soc.* **108,** 496 (1961).
17. Krier, C. A., and Jaffee, R. I., *J. Less-Common Met.* **5,** 411 (1963).
18. Chaston, J. C., *Plat. Met. Rev.* **8,** 50 (1964).
19. McCabe, R. W., Pignet, T., and Schmidt, L. D., *J. Catal.* **32,** 114 (1974).
20. Satterfield, C. N., "Heterogeneous Catalysis in Practice." McGraw–Hill, New York, 1980.
21. Bussiere, P., Devore, P., Domanski, B., and Prettre, M., "Actes du 2ieme Congr. Intern. de Catalyse," paper No. 114, p. 2247. Technip, Paris, 1962.
22. Carriere, B., Legare, P., and Maire, G., *J. Chim. Phys.* **71,** 335 (1974).
23. McCabe, R. W., and Schmidt, L. D., *Surf. Sci.* **60,** 85 (1976); **65,** 189 (1977).
24. Ducros, R., and Merrill, R. P., *Surf. Sci.* **55,** 227 (1976).
25. Matsushima, T., Almy, D. B., and White, J. M., *Surf. Sci.* **67,** 89 (1977).
26. Smith, C. E., Biberian, J. P., and Somorjai, G. A., *J. Catal.* **57,** 426 (1979).
27. Comsa, G., and Niehus, H., *Surf. Sci.* **93,** L147 (1980).
28. Bonzel, H. P., Franken, A. M., and Pirug, G., *Surf. Sci.* **104,** 625 (1981).
29. Niehus, H., and Comsa, G., *Surf. Sci.* **102,** L14 (1981).
30. Gland, J. L., *Surf. Sci.* **93,** 487 (1980).
31. Barteau, M. A., Ko, E. I., and Madix, R. J., *Surf. Sci.* **102,** 99 (1981).
32. Campbell, C. T., Ertl, G., Kuipers, H., and Segner, J., *Surf. Sci.* **107,** 220 (1981).
33. Derry, G. N., and Ross, P. N., Jr., *Surf. Sci.* **140,** 165 (1984).
34. Berry, R. J., *Surf. Sci.* **76,** 415 (1978).
35. Sales, B. C., Turner, J. E., and Maple, M. B., *Surf. Sci.* **112,** 272 (1981).
36. Turner, J. E., and Maple, M. B., *Surf. Sci.* **147,** 647 (1984).
37. Huizinga, T., Van Grondelle, J., and Prins, R., *Appl. Catal.* **10,** 199 (1984).
38. Park, S. H., Tzou, M. S., and Sachtler, W. M. H., *Appl. Catal.* **24,** 85 (1986).
39. Lieske, H., Lietz, G., Spindler, H., and Volter, J., *J. Catal.* **81,** 8 (1983).
40. Lietz, G., Lieske, H., Spindler, H., Hanke, W., and Volter, J., *J. Catal.* **81,** 17 (1983).
41. Harris, P. J. F., *J. Catal.* **97,** 527 (1986).
42. Harris, P. J. F., Boyes, E. D., and Cairns, J. A., *J. Catal.* **82,** 127 (1983).
43. Smith, D. J., White, D., Baird, T., and Fryer, J. R., *J. Catal.* **81,** 107 (1983).
44. Stulga, J. E., Wynblatt, P., and Tien, J. K., *J. Catal.* **62,** 59 (1980).
45. Lagarde, P., Murata, T., Vlaic, G., Freund, E., Dexpert, H., and Bournonville, J. P., *J. Catal.* **84,** 333 (1983).
46. Den Otter, G. J., and Dautzenberg, F. M., *J. Catal.* **53,** 116 (1978).
47. Rothschild, W. G., Yao, H. C., and Plummer, H. K., Jr., *Langmuir* **2,** 588 (1986).
48. Drozdov, V. A., Tsyrul'nikov, P. G., Popovskii, V. V., Pankrat'ev, Yu. D., Davydov, A. A., and Moroz, E. M., *Kinet. Catal.* **27,** 623 (1986). [English Transl.]
49. Wilson, G. R., and Hall, W. K., *J. Catal.* **24,** 306 (1972).
50. Glassl, H., Kramer, R., and Hayek, K., *J. Catal.* **68,** 388 (1981).
51. Wanke, S. E., and Flynn, P. C., *Catal. Rev. Sci. Eng.* **12,** 93 (1975).
52. Flynn, P. C., Wanke, S. E., and Turner, P. S., *J. Catal.* **33,** 233 (1974).
53. Baker, R. T. K., Prestridge, E. B., and Garten, R. L., *J. Catal.* **56,** 390 (1979).
54. Chen, M., and Schmidt, L. D., *J. Catal.* **55,** 348 (1978).
55. Chu, Y. F., and Ruckenstein, E., *J. Catal.* **55,** 281 (1978).
56. Harris, P. J. F., *Surf. Sci.* **185,** L459 (1987).
57. Harris, P. J. F., *Appl. Catal.* **16,** 439 (1985).
58. Kikuchi, E., Flynn, P. C., and Wanke, S. E., *J. Catal.* **34,** 132 (1974).
59. Liang, K. S., Laderman, S. S., and Sinfelt, J. H., *J. Chem. Phys.* **86,** 2352 (1987).
60. Yao, H. C., Sieg, M., and Plummer, H. K., Jr., *J. Catal.* **59,** 365 (1979).
61. Foger, K., and Jaeger, H., *J. Catal.* **70,** 53 (1981).
62. Georgopoulos, P., and Cohen, J. B., *J. Catal.* **92,** 211 (1985).
63. Kobayashi, M., Inoue, Y., Takahashi, N., Burwell, R. L., Jr., Butt, J. B., and Cohen, J. B., *J. Catal.* **64,** 74 (1980).
64. Wang, T., Lee, C., and Schmidt, L. D., *Surf. Sci.* **163,** 181 (1985).
65. Uchijima, T., Herrmann, J. M., Inoue, Y., Burwell, R. L., Jr., and Cohen, J. B., *J. Catal.* **50,** 464 (1977).
66. Sashital, S. R., Cohen, J. B., Burwell, R. L., Jr., and Butt, J. B., *J. Catal.* **50,** 479 (1977).
67. Glassl, H., Kramer, R., and Hayek, K., *J. Catal.* **63,** 167 (1980).

68. Fukushima, T., Katzer, J. R., Sayers, D. E., and Cook, J., "Proceedings, 7th International Congress on Catalysis, Tokyo, 1980," p. 79. Elsevier, Amsterdam, 1981.
69. Mills, G. A., Weller, S., and Cornelius, E. B., "Actes du 2ieme Congr. Intern. de Catalyse," paper No. 113, p. 2221. Technip, Paris, 1962.
70. Joyner, R. W., *Chem. Soc. Faraday 1* **76,** 357 (1980).
71. Bournonville, J. P., Franck, J. P., and Martino, G., "Prep. of Catalysts III" (G. Poncelet, P. Grange, and P. A. Jacobs, Eds.). Elsevier, Amsterdam, 1983.
72. Hurst, N. W., Gentry, S. J., Jones, A., and McNicol, B. D., *Catal. Rev. Sci. Eng.* **24,** 233 (1982).
73. Foger, K., and Jaeger, H., *J. Catal.* **92,** 64 (1985).
74. Isaacs, B. H., and Petersen, E. E., *J. Catal.* **77,** 43 (1982).
75. Nandi, R. K., Molinaro, F., Tang, C., Cohen, J. B., Butt, J. B., and Burwell, R. L., Jr., *J. Catal.* **78,** 289 (1982).
76. Ostermaier, J., Katzer, J., and Manogue, W. J., *J. Catal.* **41,** 277 (1976).
77. Niwa, M., Awano, K., and Murakami, Y., *Appl. Catal.* **7,** 317 (1983).
78. Scheintuch, M., and Schmitz, R. A., *ACS Symp. Ser.* **165,** 487 (1978).
79. Schmitz, R. A., *Proc. JACC* **2,** 21 (1978).
80. Vayenas, C. G., Lee, B., and Michaels, J. N., *J. Catal.* **66,** 36 (1980).
81. Vayenas, C. G., Georgakis, C., Michaels, J. N., and Tormo, J., *J. Catal.* **67,** 348 (1981).
82. Vayenas, C. G., and Michaels, J. N., *Surf. Sci.* **120,** L405 (1982).
83. Turner, J. E., Sales, B. C., and Maple, M. B., *Surf. Sci.* **103,** 54 (1981); **109,** 591 (1981).
84. Sales, B. C., Turner, J. E., and Maple, M. B., *Surf. Sci.* **114,** 381 (1982).
85. Herz, R. K., and Shinouskis, E. J., *Appl. Surf. Sci.* **19,** 373 (1984).
86. Butt, J. B., *Appl. Catal.* **15,** 161 (1985).
87. Wong, S. S., Otero-Schipper, P. H., Wachter, W. A., Inoue, Y., Kobayashi, M., Butt, J. B., Burwell, R. L., Jr., and Cohen, J. B., *J. Catal.* **64,** 84 (1980).
88. Alikina, G. M., Davydov, A. A., Sazonova, I. S., and Popovskii, V. V., *Kinet. Catal.* **27,** 758 (1987). [Engl. Transl.]
89. Yeates, R. C., Turner, J. E., Gellman, A. J., and Somorjai, G. A., *Surf. Sci.* **149,** 175 (1985).
90. Lindstrom, T. H., and Tsotsis, T. T., *Surf. Sci.* **167,** 1194 (1986).
91. Volter, J., Lietz, G., Spindler, H., and Lieske, H., *J. Catal.* **104,** 375 (1987).
92. "Catalog Handbook of Fine Chemicals," p. 901 "Aldrich Chemical Co., Milwaukee, WI, 1984–1985.
93. Wong, C., and McCabe, R. W., *J. Catal.* **107,** 535 (1987).
94. McClellan, M. R., and McFeely, F. R., *Surf. Sci.* **124,** 188 (1983).
95. Anderson, J. R., "Structure of Metallic Catalysts," p. 360. Academic Press, London/New York, 1975.
96. Cevallos Candau, J. F., and Conner, W. C., *J. Catal.* **106,** 378 (1987).
97. Hoyle, N. D., Newbatt, P. H., Rollins, K., Sermon, P. A., and Wurie, A. T., *J. Chem. Soc. Faraday Trans. 1* **81,** 2605 (1985).
98. Wagstaff, N., and Prins, R., *J. Catal.* **59,** 434 (1979).